

Supporting Information

Na Yang, Li Li, Jing Li and Zidong Wei**

School of Chemistry and Chemical Engineering, Chongqing University, Shazhengjie
174, Chongqing 400044, China

*Corresponding author's E-mail: liliracial@cqu.edu.cn; zdwei@cqu.edu.cn, Tel: +86
2365678945

Keywords: doped phosphorene, nonmetallic dopants, stability, sensibility

*Corresponding author's E-mail: liliracial@cqu.edu.cn; zdwei@cqu.edu.cn, Tel: +86
2365678945

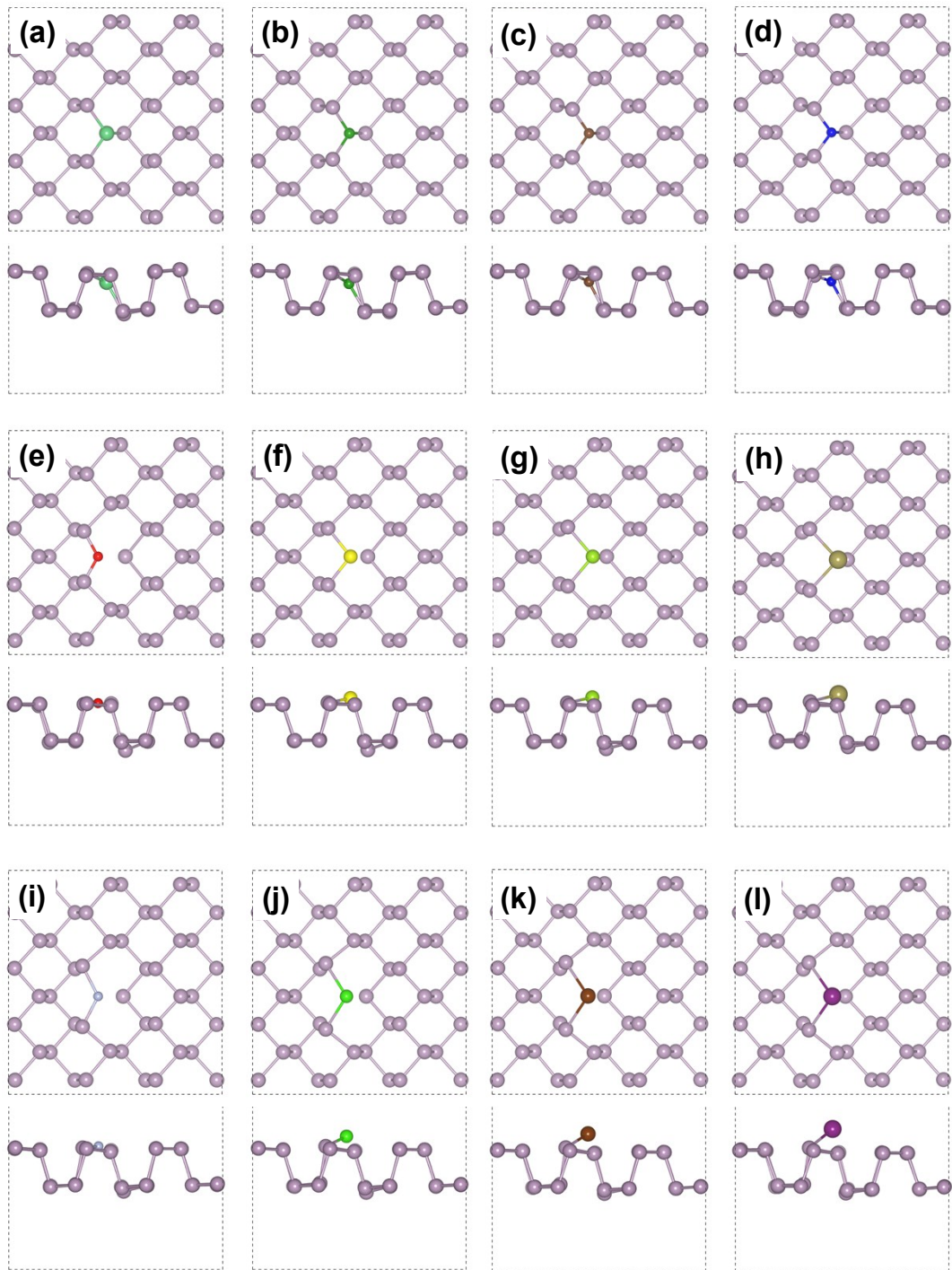


Figure S1. Optimized supercell structures for the different models of X-doped phosphorene (top and side views): (a) Be-, (b) B-, (c) C-, (d) N-, (e) O-, (f) S-, (g) Se-, (h) Te-, (i) F-, (j) Cl-, (k) Br- and (l) I-doped phosphorene. The pink, reseda, dark green, brownness, blue, red, yellow, cyan, brown, silver, green, dark brown and purple spheres represent the P, Be, B, C, N, O, S, Se, Te, F, Cl, Br and I atoms, respectively.

Table S1. The bond lengths, atomic radius, formation energy, binding energy and fermi energy of the investigated models.

Model	Bond lengths /Å				$R_{P/X}$ /Å	$E_{\text{formation}}$ / eV	$E_{\text{binding}} /$ eV	$E_{\text{Fermi}} /$ eV
	d_{X-P_1}	d_{X-P_2}	d_{X-P_3}	$d_{P_1-P_4}$				
phosphorene	2.22	2.23	2.22	3.21	1.06	0	-5.45	-1.02
Be-doped phosphorene	2.10	2.13	2.10	3.20	0.90	-1.19	-5.17	-1.42
B-doped phosphorene	1.94	1.91	1.94	3.35	0.82	0.85	-7.78	-1.13
C-doped phosphorene	1.80	1.81	1.80	3.33	0.77	-1.75	-8.22	-1.36
N-doped phosphorene	1.78	1.80	1.78	3.21	0.75	0.58	-6.62	-1.08
O-doped phosphorene	1.71	3.24	1.71	3.06	0.73	-0.87	-6.29	-1.05
S-doped phosphorene	2.17	3.25	2.17	3.17	1.02	0.67	-4.56	-1.04
Se-doped phosphorene	2.32	3.15	2.32	3.22	1.16	1.11	-3.91	-1.01
Te-doped phosphorene	2.52	3.15	2.52	3.28	1.36	1.42	-3.29	-0.88
F-doped phosphorene	2.03	3.14	2.03	3.16	0.72	-0.40	-3.77	-1.13
Cl-doped phosphorene	2.38	3.61	2.38	3.25	0.99	1.39	-2.17	-0.98
Br-doped phosphorene	2.51	3.80	2.51	3.30	1.14	1.60	-1.70	-0.96
I-doped phosphorene	2.69	4.13	2.69	3.36	1.33	1.53	-1.23	-0.88

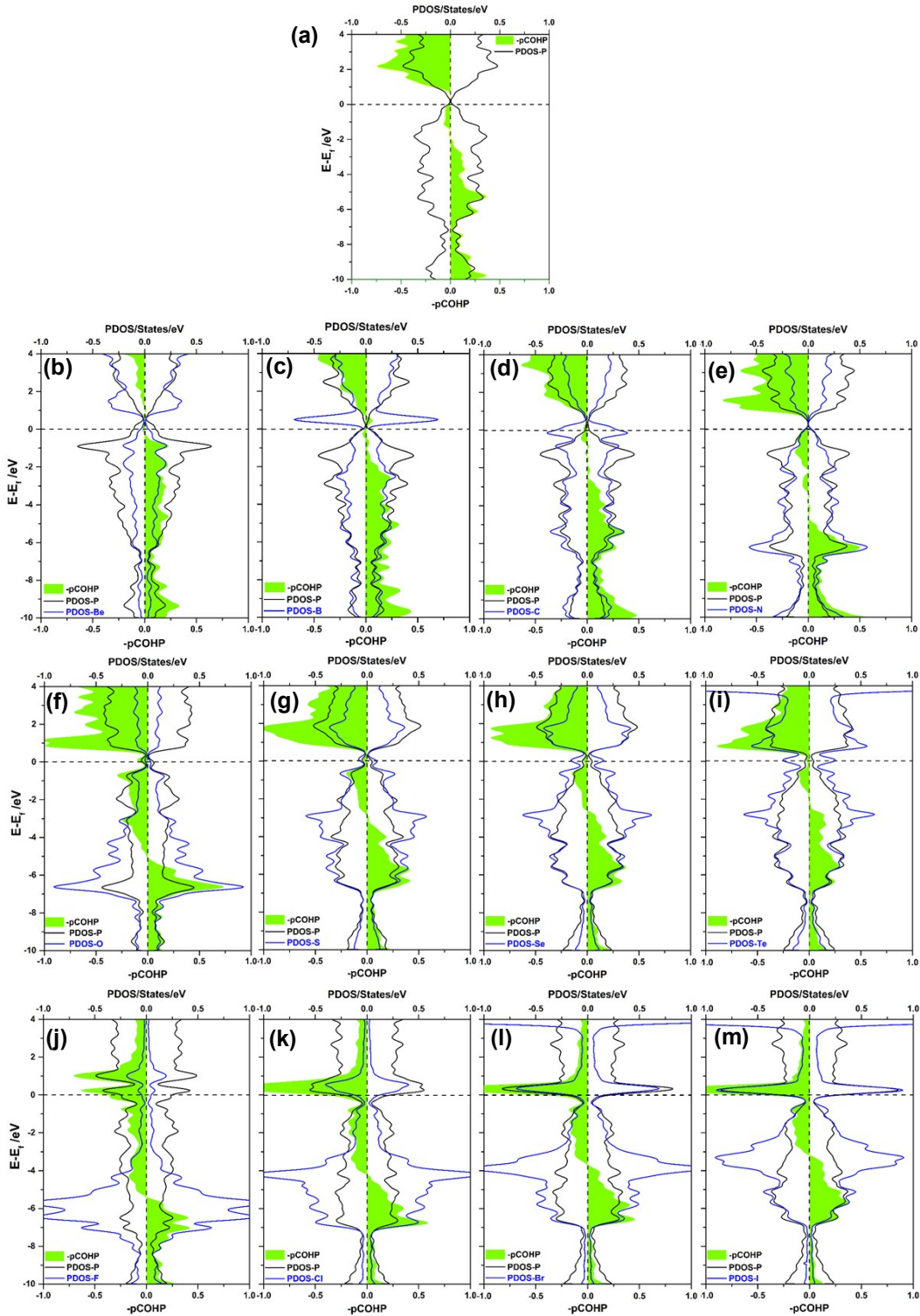


Figure S2. The partial density of states (PDOS) and projected crystal orbital Hamilton population (pCOHP) curves for the X-P₁ interaction in different X-doped phosphorene system: (a) pure phosphorene, (b) Be-, (c) B-, (d) C-, (e) N-, (f) O-, (g) S-, (h) Se-, (i) Te-, (j) F-, (k) Cl-, (l) Br- and (m) I-doped phosphorene. The bonding (stabilizing) contributions are visualized on the right side of the energy axis, and the antibonding (destabilizing) ones are on the other side.

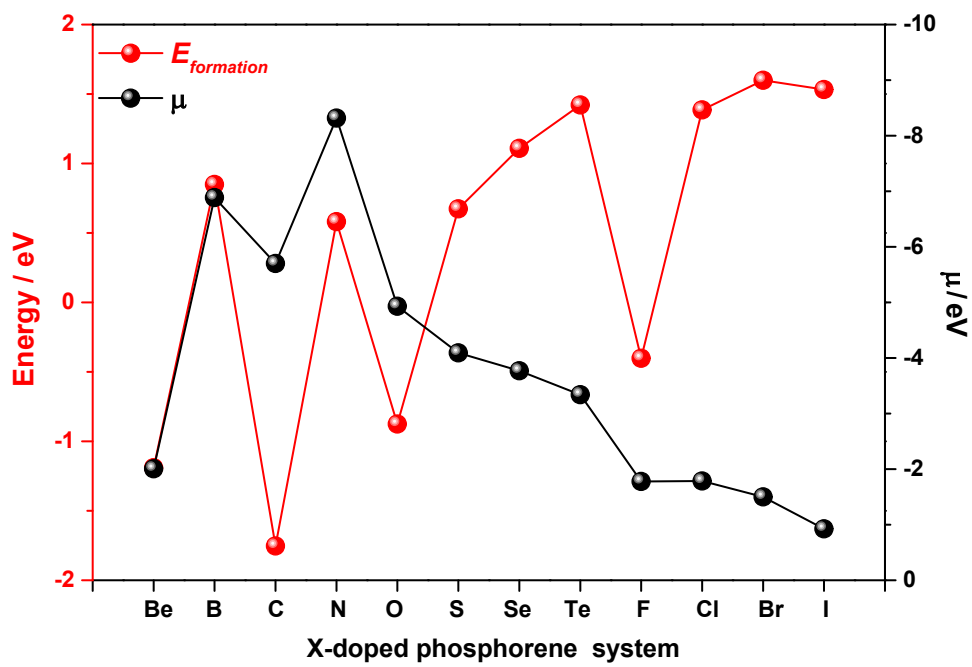


Figure S3. The formation energy ($E_{formation}$) of X-doped phosphorene models and chemical potential (μ) of X atoms.

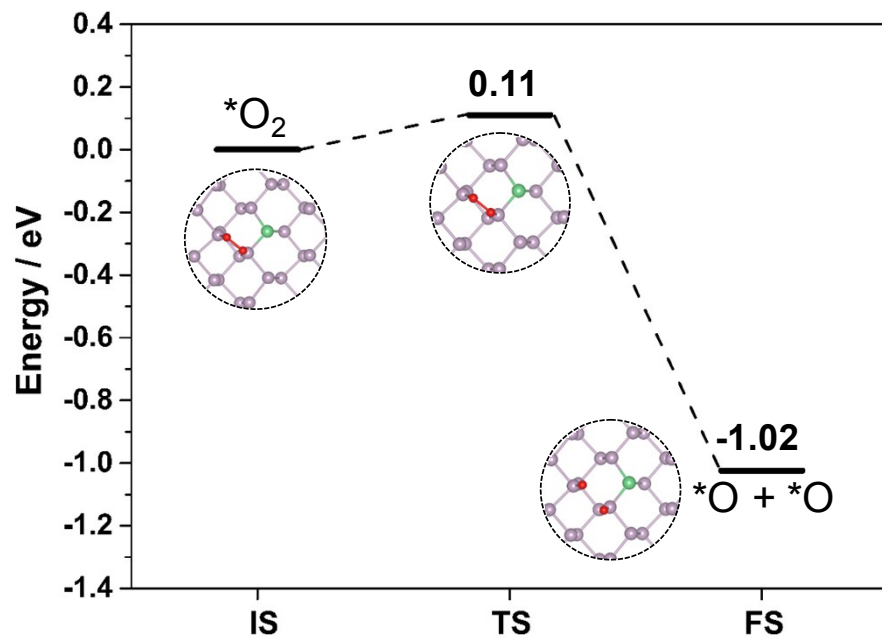


Figure S4. The energy profile of $*\text{O}_2$ dissociation on Be-doped phosphorene surface.

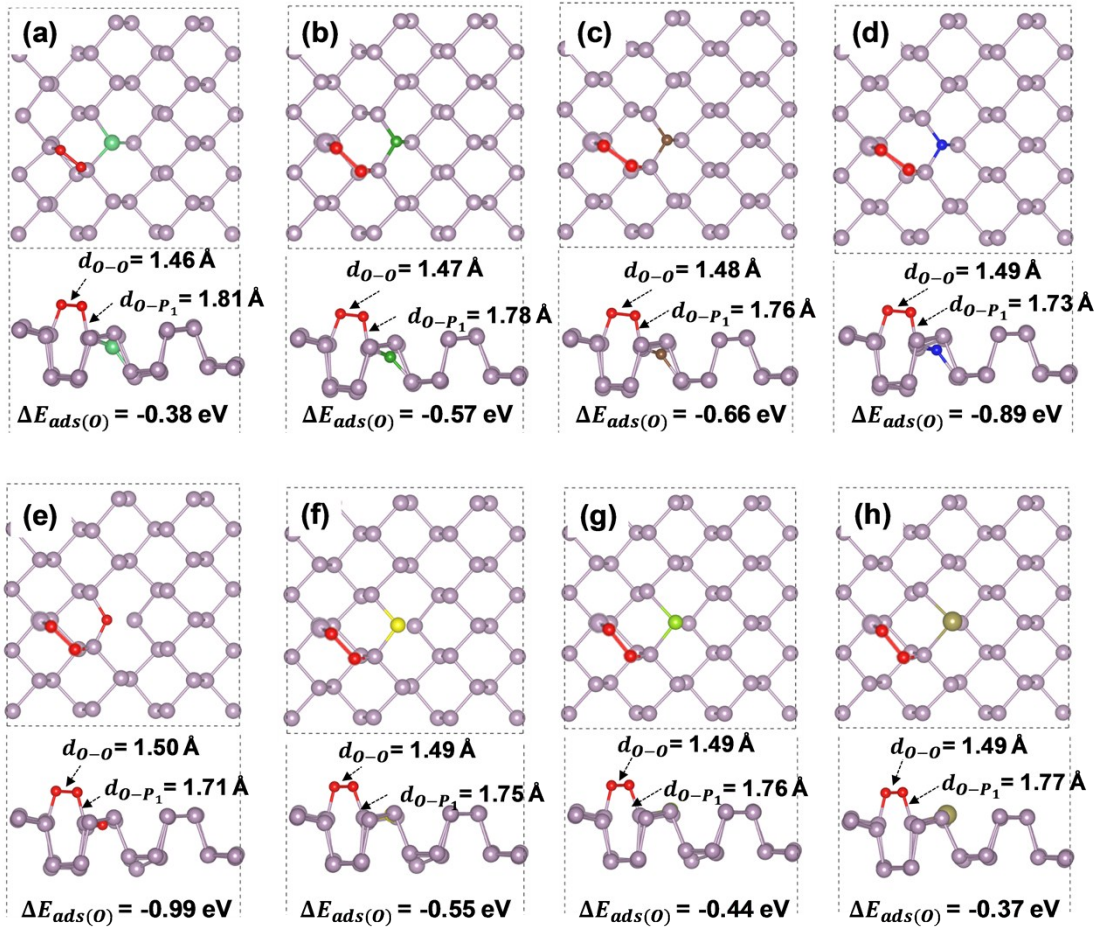


Figure S5. The $*\text{O}_2$ adsorption configurations on the different models of X-doped phosphorene (top and side views): (a) Be-, (b) B-, (c) C-, (d) N-, (e) O-, (f) S-, (g) Se- and (h) Te-doped phosphorene.

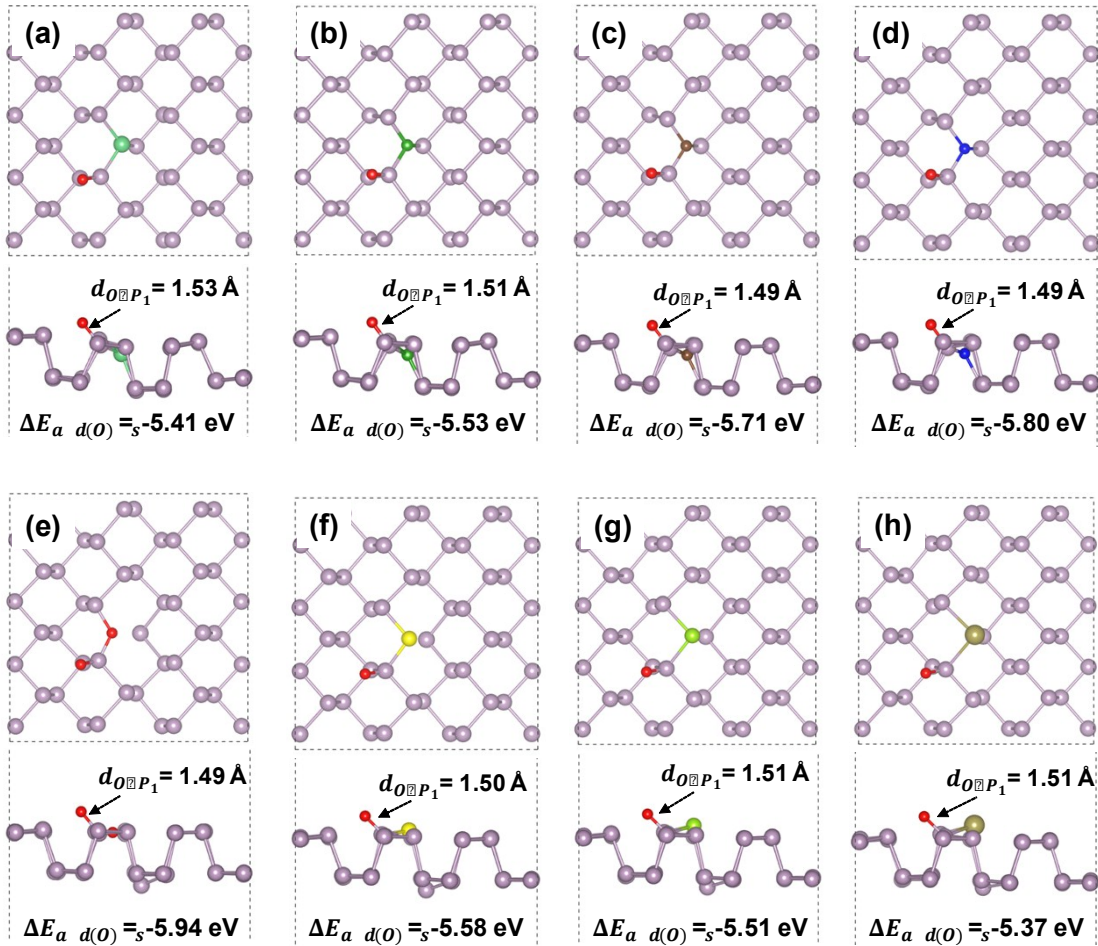


Figure S6. The $*\text{O}$ adsorption configurations on the different models of X-doped phosphorene (top and side views): (a) Be-, (b) B-, (c) C-, (d) N-, (e) O-, (f) S-, (g) Se- and (h) Te-doped phosphorene.

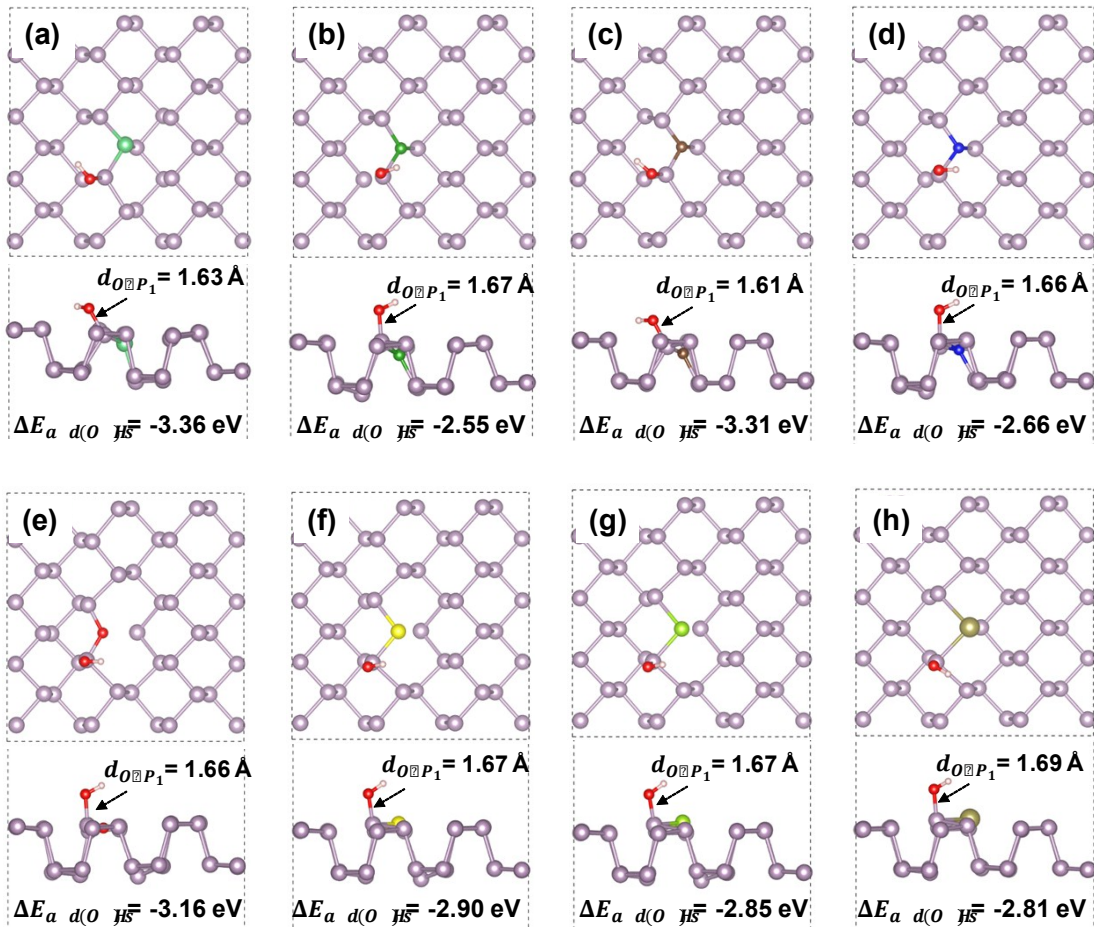


Figure S7. The $^*\text{OH}$ adsorption configurations on the different models of X-doped phosphorene (top and side views): (a) Be-, (b) B-, (c) C-, (d) N-, (e) O-, (f) S-, (g) Se- and (h) Te-doped phosphorene.

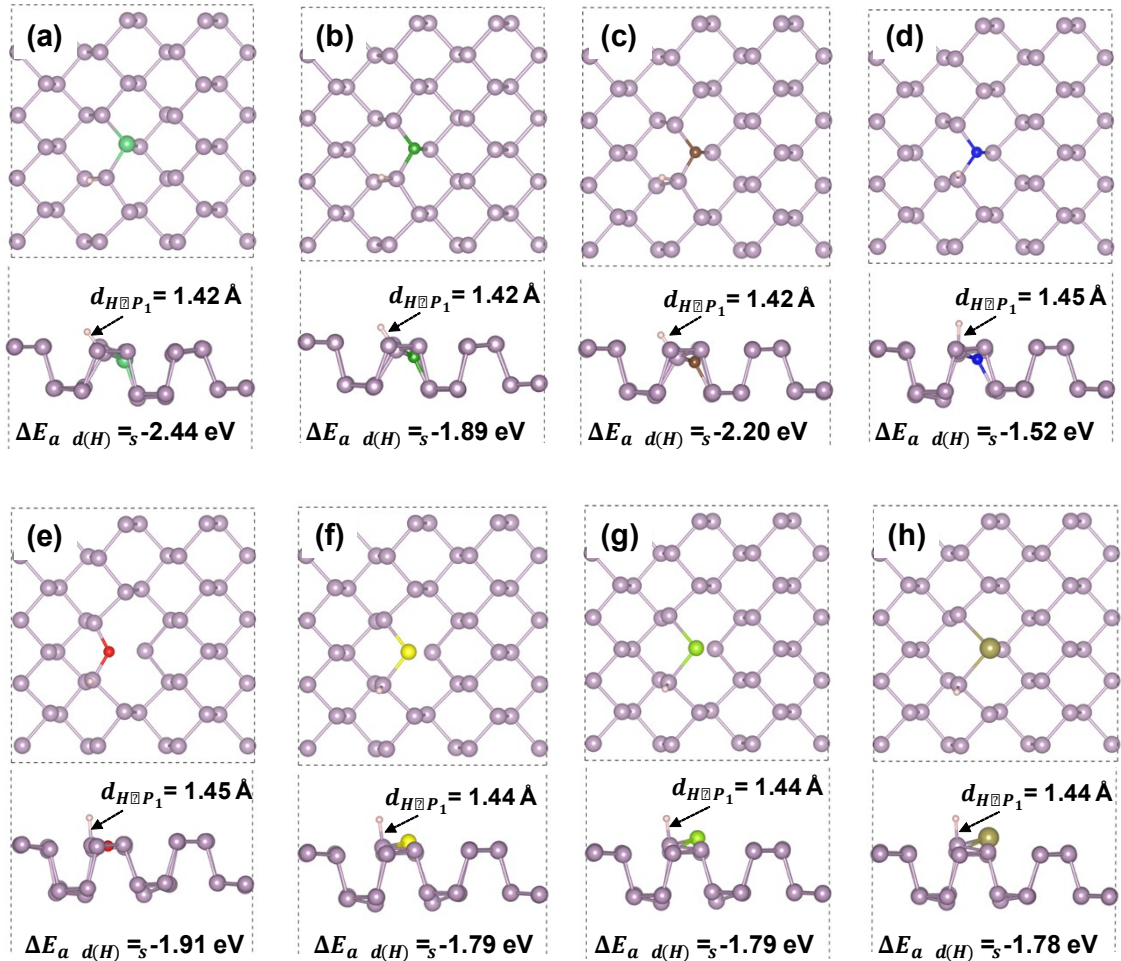


Figure S8. The $^*\text{H}$ adsorption configurations on the different models of X-doped phosphorene (top and side views): (a) Be-, (b) B-, (c) C-, (d) N-, (e) O-, (f) S-, (g) Se- and (h) Te-doped phosphorene.

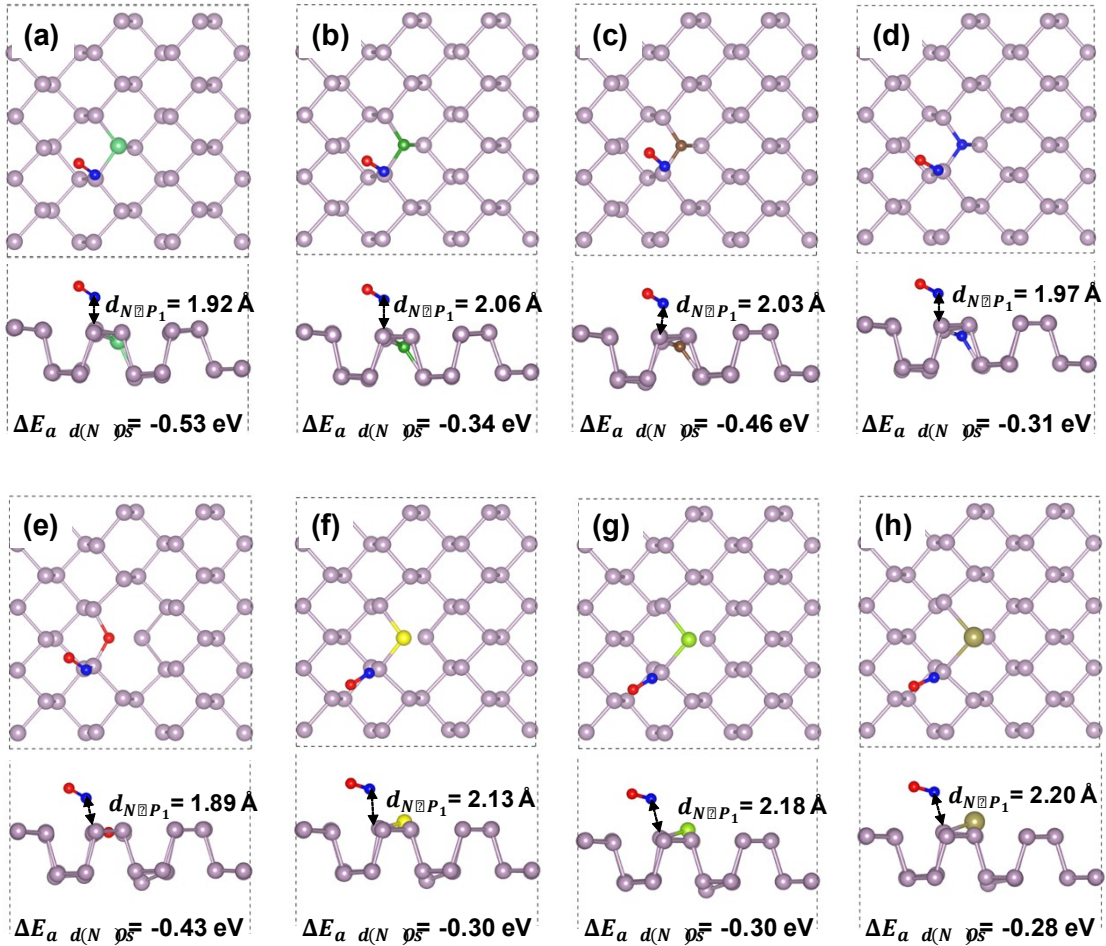


Figure S9. The *NO adsorption configurations on the different models of X-doped phosphorene (top and side views): (a) Be-, (b) B-, (c) C-, (d) N-, (e) O-, (f) S-, (g) Se- and (h) Te-doped phosphorene.

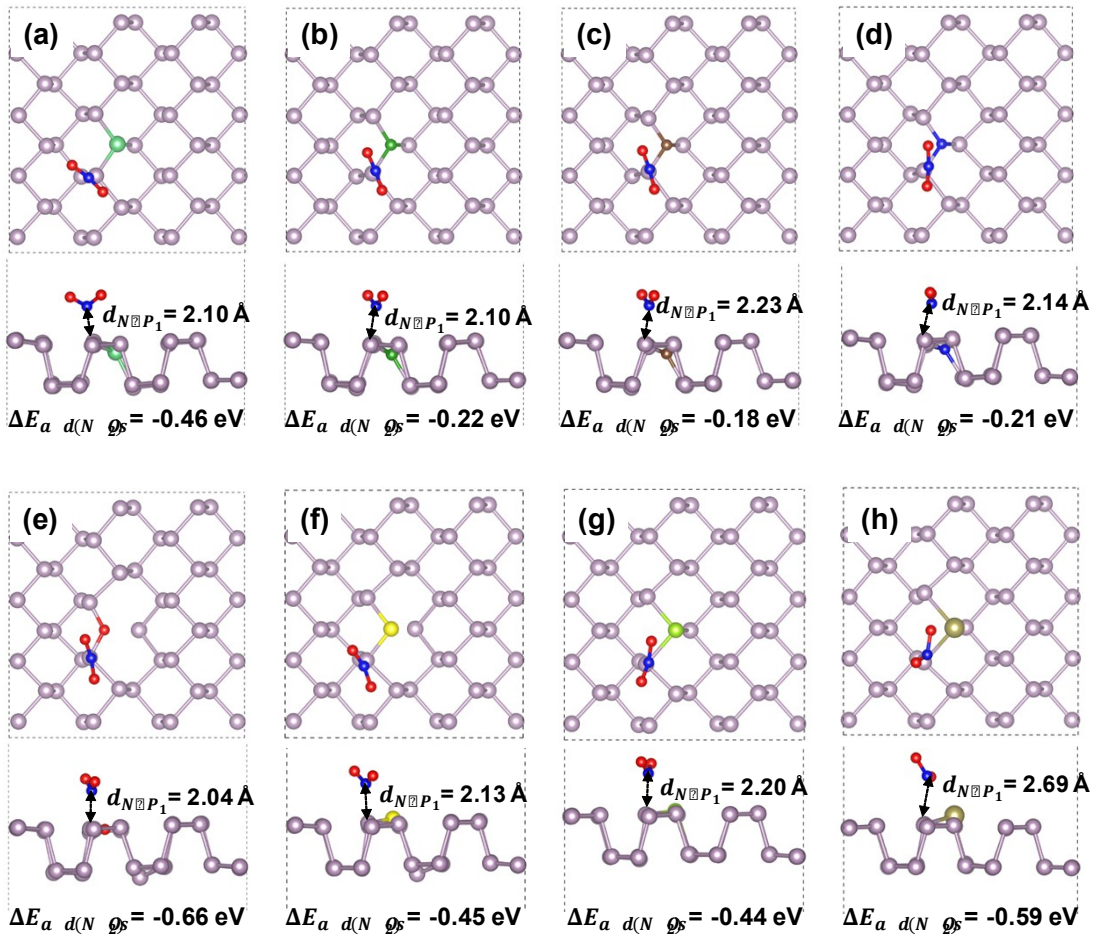


Figure S10. The $*\text{NO}_2$ adsorption configurations on the different models of X-doped phosphorene (top and side views): (a) Be-, (b) B-, (c) C-, (d) N-, (e) O-, (f) S-, (g) Se- and (h) Te-doped phosphorene.

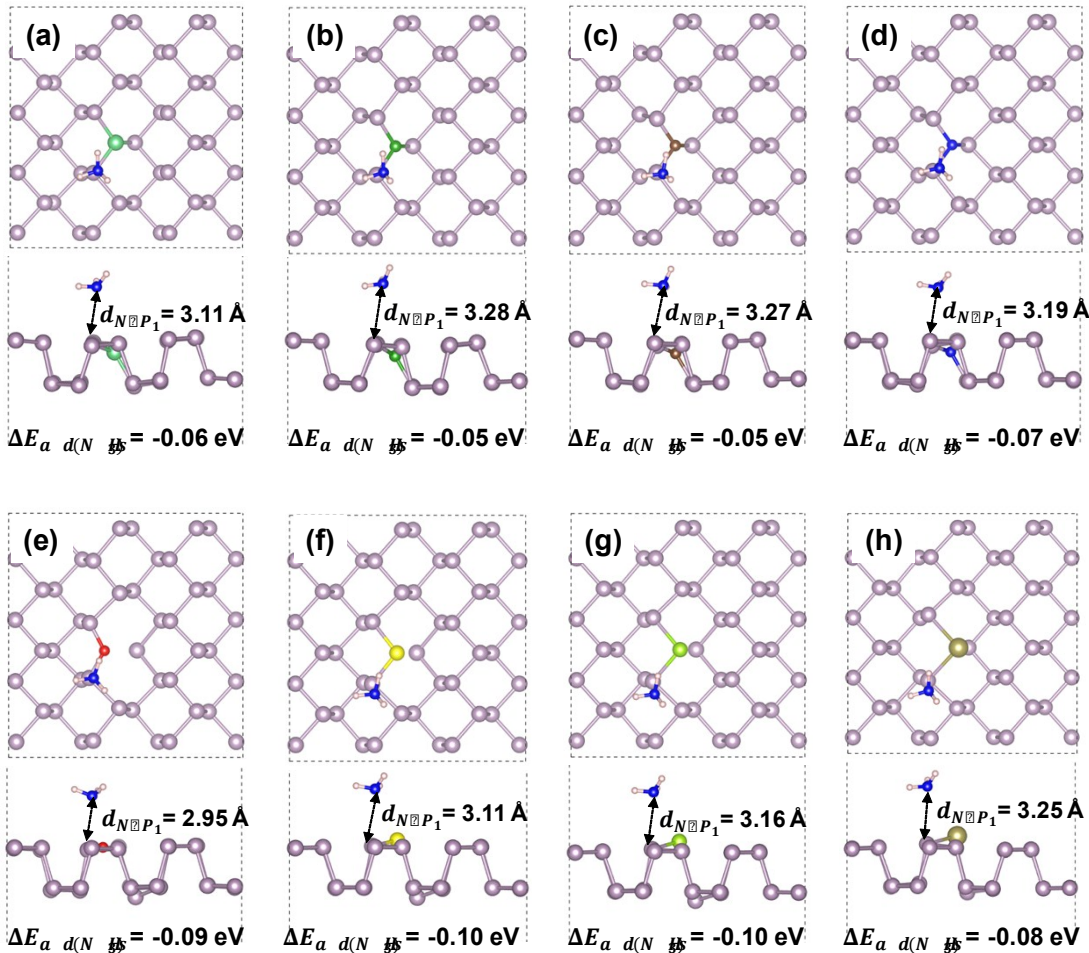


Figure S11. The $^*\text{NH}_3$ adsorption configurations on the different models of X-doped phosphorene (top and side views): (a) Be-, (b) B-, (c) C-, (d) N-, (e) O-, (f) S-, (g) Se- and (h) Te-doped phosphorene.

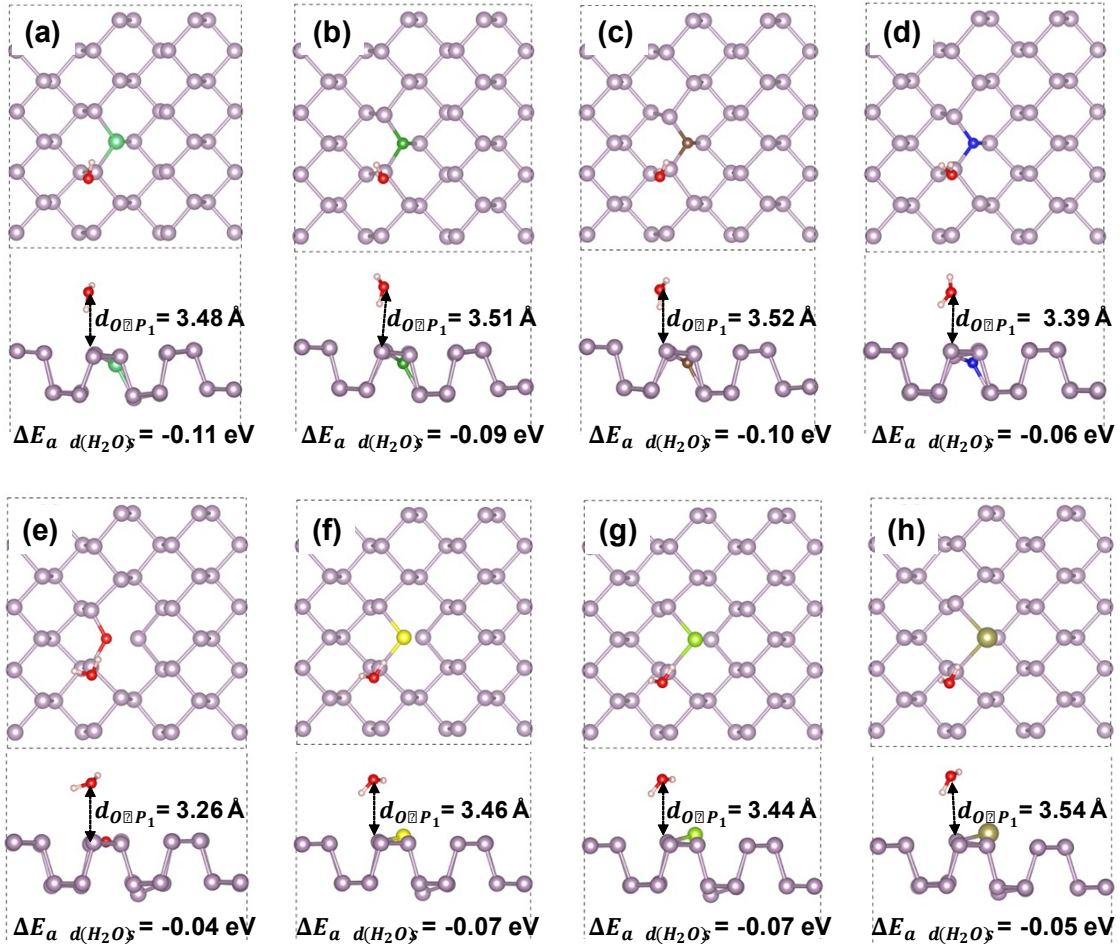


Figure S12. The $*\text{H}_2\text{O}$ adsorption configurations on the different models of X-doped phosphorene (top and side views): (a) Be-, (b) B-, (c) C-, (d) N-, (e) O-, (f) S-, (g) Se- and (h) Te-doped phosphorene.

Table S2. The charge transfer (ΔQ_P) data on phosphorene surface when the species are charged ion or neutral atoms.

Adsorption Species	O	O^{2-}	OH	OH^-	H	H^+
$\Delta Q_P/\text{e}$	1.12	1.13	0.76	0.71	0.35	0.35

ΔQ_P : The amount charge transfer between the P atoms and adsorption species

Table S3. The adsorption energies of investigated species on the X-doped phosphorene.

Model	Adsorption Energy / eV							
	* O ₂	* O	* OH	* H	* NO	* NO ₂	* NH ₃	* H ₂ O
phosphorene	-0.60	-5.44	-2.5	-1.53	-0.20	-0.17	-0.07	-0.05
Be-doped phosphorene	-0.38	-5.41	-3.36	-2.44	-0.53	-0.46	-0.06	-0.11
B-doped phosphorene	-0.57	-5.53	-2.55	-1.89	-0.34	-0.22	-0.05	-0.09
C-doped phosphorene	-0.66	-5.71	-3.31	-2.20	-0.46	-0.18	-0.05	-0.10
N-doped phosphorene	-0.89	-5.80	-2.66	-1.52	-0.31	-0.21	-0.07	-0.06
O-doped phosphorene	-0.99	-5.94	-3.16	-1.91	-0.43	-0.66	-0.09	-0.04
S-doped phosphorene	-0.55	-5.58	-2.90	-1.79	-0.30	-0.45	-0.10	-0.07
Se-doped phosphorene	-0.44	-5.51	-2.85	-1.79	-0.30	-0.44	-0.10	-0.07
Te-doped phosphorene	-0.37	-5.37	-2.81	-1.78	-0.28	-0.59	-0.08	-0.05